Molecular Packing of Long-Chain *n*-Alkanes in the MCM-41 Nanochannel As Probed by the Free Radicals Produced by γ-Irradiation

Kazumi Toriyama* and Masaharu Okazaki*

Institute for Advanced Science and Technology, Instrumentation Frontier Institute, 2266-98 Shimoshidami, Moriyama-ku, Nagoya 463-8560, Japan

Received: March 25, 2004; In Final Form: June 16, 2004

The physical states of long-chain *n*-alkane molecules in the nanochannel of MCM-41, a mesoporous silica, were studied by observing the ESR spectra of alkyl radicals formed by radiolysis. The ESR spectra for the systems with *n*-decane, *n*-undecane, *n*-dodecane, or *n*-tridecane, which were confined in the MCM-41 nanochannel and irradiated with γ-rays at 77 K, were almost identical. Since the ESR spectra for the irradiated *n*-alkane crystals, which are due to the three types of radicals, R_I ($^{\bullet}CH_2CH_2R$), R_{II} ($CH_3{}^{\bullet}CHCH_2R'$), and R_{III} ($RCH_2{}^{\bullet}CHCH_2R''$), change alternatively as the carbon number changes consecutively, the above results suggest that these *n*-alkanes are solidified in a similar way and cannot form regular crystals in the nanochannel. A model is proposed for the molecular packing from the dynamics, the relative yields of these three radicals, which do not deviate largely from those for *n*-undecane and *n*-tridecane crystals, and their temperature dependencies.

1. Introduction

Many studies have been made on the chemical reactions in the nanopore after the emergence of ZMS, a high-silica zeolite.[1] The reactions proceed stereospecifically in the pore with a diameter less than 1.0 nm. The Broensted and Lewis acid points at the Al^{3+} ions work as the active sites.[2] On the contrary, MCM-41 is a stack of nanochannels 2−10 nm in diameter and is made of SiO_2 only;[3] therefore, another type of reaction process may be expected within this nanospace. We have been studying the nanospace effects for several liquid-phase photochemical reactions in the MCM-41 channel and observed large magnetic-field effects in the product yields.[4] This effect could be explained successfully by the "radical pair mechanism", which has been used to explain the magnetic-field-dependent reactions in micelle, which include the radical pairs as the intermediates.[5] From these results, we proposed a model in which (1) the solution flows in the nanochannel of MCM-41, even at a pressure that is usually employed in liquid chromatography, and (2) the solution molecules flow as a group without mixing with the neighboring molecules for more than a few microseconds.[6,7] These two postulations, however, contradict the usual solution dynamics in the classical model. According to Poiseuille's law, molecules near the tube center flow much faster than those near the tube wall. The time calculated by Poiseuille's law is several thousand times longer than the observed time required for the solution to flow through the MCM-41 nanochannel.[8] In addition, the classical diffusion model expects that the solution molecules frequently change their order during the flow in the nanochannel. Therefore, to explain the above observations, a completely new model is necessary for the dynamic behavior of liquids in the nanochannel.

Much work on the physical state of water in the nanospace has been carried out by means of NMR, DSC, XRD, and so forth.[9−11] It has been reported that the freezing temperature of water is lowered in the micropore. It is very important to know how the nonpolar molecules, such as alkanes, act in the nanospace to clarify the basic feature of the molecules in the nanospace. The aim of the present study is to clarify the physical features of *n*-alkane molecules in the nanochannel of the mesoporous silica, MCM-41, and to compare them with those in the bulk state. We observed, by means of the ESR (electron spin resonance) technique at 77 K, the free radicals, which were produced by γ-irradiation as the probe of the *n*-alkanes that were confined and frozen in the nanochannel of MCM-41.

When *n*-alkanes are irradiated with γ-rays at 77 K, three types of alkyl radicals, $^{\bullet}CH_2CH_2R$ (R_I), $CH_3{}^{\bullet}CHCH_2R'$ (R_{II}), and $RCH_2{}^{\bullet}CHCH_2R''$ (R_{III}), are formed. It has been found that the relative populations of the three types of alkyl radicals observed in the polycrystalline samples largely differ between the two groups of *n*-alkanes: one with an even number of carbons (called even *n*-alkane, hereafter) and the other with an odd number of carbons (odd *n*-alkane). That is, the R_I radical is the most populated in the orthorhombic crystal of an odd *n*-alkane, while R_{II} is the major radical in the triclinic crystal of an even *n*-alkane. As a result, the appearance of the ESR spectra of a series of *n*-alkanes changes alternatively depending on the number of carbons in the molecule (n_C).[12] This is the result of radical site migration from R_I to R_{II} during the radiolysis, which is much easier in the triclinic crystals compared with that in the orthorhombic crystals. This comes from the specific nature of a radical reaction in the low-temperature solid that is highly dependent on the molecular arrangement in the crystal.[13] Thus, the alkyl radicals that are produced by the X- or γ-irradiation of *n*-alkanes at 77 K are good probes for investigating the physical states of these alkanes.

2. Experimental Section

Following the literature, MCM-41 was synthesized from tetraethoxysilane (TEOS) by the aid of a "template" that was produced with cetyltrimethylammonium bromide (CTAB) or

* Corresponding authors: K.T. Tel.: +81-52-7367138. Fax: +81-736-7405. E-mail: k-toriyama@aist.go.jp. M.O. Tel.: +81-52-7367138. Fax: +81-736-7405. E-mail: masa-okazaki@aist.go.jp.

10.1021/jp048662o CCC: $27.50
Published on Web 07/24/2004

decyltrimethylammonium bromide (DTAB).[14] The chain length of the adopted template molecule is indicated in parentheses, for example, as MCM-41(16) in the case of CTAB. The diameter of the nanochannel of calcined MCM-41(16) was determined to be 3.8 nm from the lattice constant of 4.5 nm, obtained by XRD analysis, and the surface area of 900 m^2/g which was determined by the one-point BET method. A 2.6 nm diameter was obtained for MCM-41(10) by the same procedure from a lattice constant of 3.2 nm and a surface area of 1000 m^2/g. The particle size was around 5 μm, according to the SEM observations. Both MCM-41(16) and MCM-41(10) adsorbed ca. 1.0 mL/g of *n*-decane at the ambient temperature of ca. 298 K.

TEOS, CTAB, and DTAB were obtained from Aldrich. *n*-Decane, *n*-undecane, *n*-dodecane, and *n*-tridecane were obtained as the standard samples for gas chromatography from Tokyo Kasei Kogyo Company. All of these chemicals were used without further purifications.

Samples for the ESR measurements were prepared as follows. Approximately 0.1 g of MCM-41 in a spherical Pyrex vessel, which was connected to the ESR sample tube, was dehydrated at 400 K for more than 10 h in air and then degassed at the same temperature for more than 1 h under vacuum ($<10^{-4}$ mmHg). Then, approximately 0.1 mL of *n*-alkane was injected via the septum to the vessel containing MCM-41 and deoxygenated by the pump-and-thaw cycles. After waiting for ca. 24 h at the ambient temperature, we transferred the MCM-41 powder to the ESR sample tube. Since all of the solvent exists in the nanochannel and the outer surface of the MCM-41 particle is dry at this stage, it can be transferred easily to the ESR tube. Nevertheless, the alkane molecules in the MCM-41 channel exist in the liquid state at the ambient temperature. This was confirmed by observing the ESR spectrum of a spin probe, $((CF_3)_2FC)_3C^{\bullet}$,[15] that was dissolved in *n*-tridecane. The prepared samples were kept frozen for 3 h or more at 77 K and irradiated with ^{60}Co γ-rays at the same temperature for 0.5 h at the dose rate of 10 kGy/h. In some cases, a few torr of N_2 gas was introduced into the system as the thermal medium to confirm that precooling for 3 h was enough, even without the thermal medium.

3. Results

Figure 1a−d shows the ESR spectra for the MCM-41(16) systems containing *n*-decane, *n*-undecane, *n*-dodecane, and *n*-tridecane, respectively, irradiated at 77 K and observed at the same temperature. All of these ESR spectra are quite similar to each other and are composed of eight lines with line widths of about 1.5 mT. On the other hand, corresponding spectra for these alkanes in the polycrystalline state change their shapes alternately as shown in Figure 1f−i. The small differences between the two groups (odd alkanes, Figure 1b and d, and even alkanes, Figure 1a and c) are interpreted as the result of small amounts of polycrystalline parts. When the space between the MCM-41 particles is also filled with the excess solvent, the superposition of the polycrystalline spectrum increases for both groups of alkanes. Thus, it is concluded that the spectra seen in Figure 1a−d are characteristic of the *n*-alkanes that are confined in the nanochannel; therefore, the physical states of those *n*-alkanes in the nanochannel are different from those in the bulk samples.

No appreciable spectral changes were observed for any of the samples upon increasing the temperature to 135 K. At temperatures above 155 K, however, the radical centers decay gradually and the spectra approach the corresponding ones of the bulk samples. The total radical concentrations at this stage are around 25−30% of those immediately after irradiation. Further appreciable decrease in the radical concentration was not observed below 200 K. Essentially, the same results were obtained for the samples included in MCM-41(10). In this case, the differences in the spectral features between *n*-decane and *n*-undecane at 77 K were smaller and the amounts of surviving radicals after the treatment at 200 K were also smaller than those in MCM-41(16). These results indicate that a small part of *n*-alkanes freezes in the normal polycrystalline state in the small central part of the MCM-41 channel and that the major part is in the "disordered state". The latter state will be discussed in a later section. As mentioned above, the alkyl radicals that formed in the disordered state are considerably unstable. On the other hand, the alkyl radicals in the polycrystalline part are stable below 200 K both in the bulk sample and in the MCM-41 nanochannel.

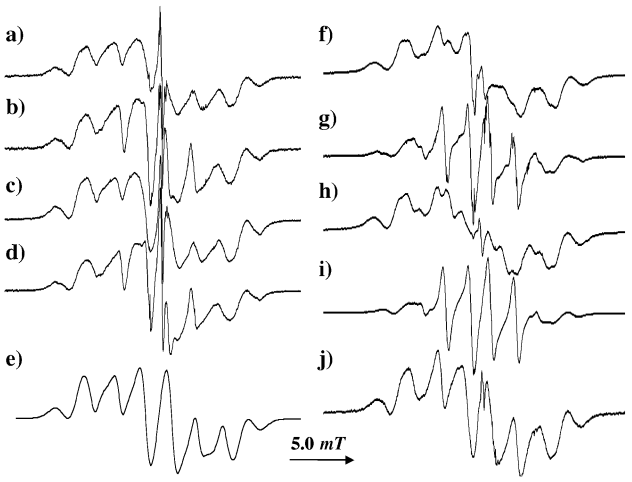

Figure 1. ESR spectra for the *n*-$C_{10}H_{22}$ (a and f), *n*-$C_{11}H_{24}$ (b and g), *n*-$C_{12}H_{26}$ (c and h), and *n*-$C_{13}H_{28}$ (d and i) systems after γ-irradiation at 77 K and observed at the same temperature: (a−d) in MCM-41(16) and (f−i) in the bulk solids. (e) Simulation for (a−d), assuming superposition of three types of alkyl radicals (see text). (j) Spectrum observed for the equimolar mixture of *n*-$C_{10}H_{22}$, *n*-$C_{11}H_{24}$, *n*-$C_{12}H_{26}$, and *n*-$C_{13}H_{28}$. Both γ-irradiation and ESR observation were performed at 77 K.

Spectral simulation was performed for the broad eight-line spectrum observed in the long-chain *n*-alkanes irradiated in the MCM-41 channel, assuming that the spectrum is composed of the three types of radicals, R_I ($^{\bullet}CH_2CH_2-$), R_{II} ($CH_3{}^{\bullet}CHCH_2-$), and R_{III} ($-CH_2{}^{\bullet}CHCH_2-$). The result is shown as Figure 1e. For the component spectra of R_{II} and R_{III}, the same parameters reported for the corresponding radicals in the polycrystalline samples are adopted, except for the component line width of 0.8 mT, which is a little wider than those previously reported (0.5−0.7 mT).[12,13] For R_I, on the other hand, the parameters listed in Table 1 are used. The modified Bloch's equation for the two-site exchange was applied for the restricted 180° reorientation of the CH_2 group. With the same equation and hfc tensors for the two α-protons, the spectrum of R_I in the bulk polycrystalline *n*-undecane was well reproduced with a τ value of 5×10^{-11} s. In previous works on the bulk systems,[12,13] Iwasaki et al. obtained the same simulated spectrum by the usual static simulation with the average hfc tensor for the α-protons (Table 1).

Finally, the observed spectrum was simulated satisfactorily by superposing the spectra of R_I, R_{II}, and R_{III} with the ratio of 0.47:0.26:0.27. This fraction is practically common to all of the four *n*-alkane systems in MCM-41, indicating that alkyl

TABLE 1: ESR Parameters Adopted for the Spectrum Simulation of Terminal Alkyl Radicals (R_I) Formed from Long-Chain *n*-Alkane γ-Irradiated at 77 K[a]

	α-H		β-H			
radical environment	A_{ii} (mT)	directions in molecular axis	$a(H_1)$ (mT)	$a(H_2)$ (mT)	ΔH (mT)	τ^b (s^{-1})
n-C_mH_{2m+2}	−1.17	∥ C−H	3.9	2.5	0.8	5.0×10^{-8}
($m = 10-13$)	−1.96	⊥ CH_2 plane				
in MCM-41	−3.52	⊥ C−H in plane				
polycrystalline	−1.76	⊥ C−C in plane	3.6	2.1	0.5	
n-undecane[c]	−1.96	⊥ CH_2 plane				
	−2.90	∥ C−C				

[a] The anisotropy of the **g**-tensor is neglected. [b] Correlation time. [c] From ref 13. This hyperfine coupling tensor can be obtained by averaging the two hyperfine tensors of the α-protons in MCM-41.

TABLE 2: Relative Yield of Three Types of Alkyl Radicals in Long-Chain *n*-Alkane γ-Irradiated at 77 K

	R_I	R_{II}	R_{III}	reference
in MCM-41 *n*-C_mH_{2m+2} ($m = 10-13$)	0.47	0.27	0.26	this work
polycrystalline *n*-tridecane	0.45	0.10	0.45	13
polycrystalline *n*-dodecane	0.06	0.52	0.42	13

radicals are trapped in almost the same ratio in the disordered region for all of the systems. In the case of the polycrystalline state at 77 K, however, a similar composition for the three types of alkyl radicals is observed for the odd *n*-alkanes but not for the even *n*-alkanes[13] (see Table 2).

4. Discussions

Characteristic features of the free radicals that are produced in *n*-alkanes which are frozen in the MCM-41 nanochannels include the following: (1) a large amount of R_I is stabilized for the even *n*-alkanes, as well, (2) the reorientation of the terminal $^{\bullet}CH_2$ group of R_I radicals is highly restricted, and (3) the onset temperature for radical decay is around 50 K lower than that in the bulk system. In the bulk system irradiated at 77 K, a large amount of R_I radical is produced only in the odd *n*-alkanes, as mentioned above. The absence of R_I in the even *n*-alkanes has been interpreted as being a result of the radical site migration from R_I to R_{II}, though the primary event occurs at the chain end to yield R_I selectively.[16,17] In the triclinic crystal of the even homologues, one of the C_2-H bonds of the neighboring molecules is directed to the unpaired electron orbital of the R_I radical. Therefore, R_I abstracts the proton of this C_2-H easily, and R_{II} is formed. Since H abstraction at the low temperature is strongly dependent on the distance and relative orientation of the reactant molecules, this reaction is impossible not only in the orthorhombic crystal of the odd *n*-alkanes but also in a distorted triclinic structure. The observation that a large amount of R_I is stably trapped in the even *n*-alkanes included in the MCM-41 nanochannel indicates that these alkanes cannot form the normal triclinic crystal in the nanochannel.

The fact that the terminal CH_2 group of the R_I radical is extremely immobilized indicates that *n*-alkanes also cannot form the normal orthorhombic crystals in the channel of MCM-41. As mentioned in the previous section, the terminal HCH group of R_I reorients rapidly in the odd *n*-alkane crystals not only at 77 K but also at 4.2 K[12,13] (see Table 1). In MCM-41, however, this dynamic is considerably suppressed even at 77 K. The apparent conformation of two β-protons (18°, 41°), with $B_2 = 4.5$ mT (see Figure 2), is derived from the well-known "$\cos^2\theta$" rule on the assumption that the HCH dihedral angle is 120°. This does not deviate much from that of polycrystalline *n*-undecane (17°, 43°), and $B_2 = 4.1$ mT. A slightly larger B_2 value in the MCM-41 system indicates that some reduction occurs on the oscillation around the C−C bond (see Figure 2).[12] Thus, these observations on the β-proton hfc tensor also indicate that molecular dynamics of the R_I radical is restricted considerably in the nanochannel.

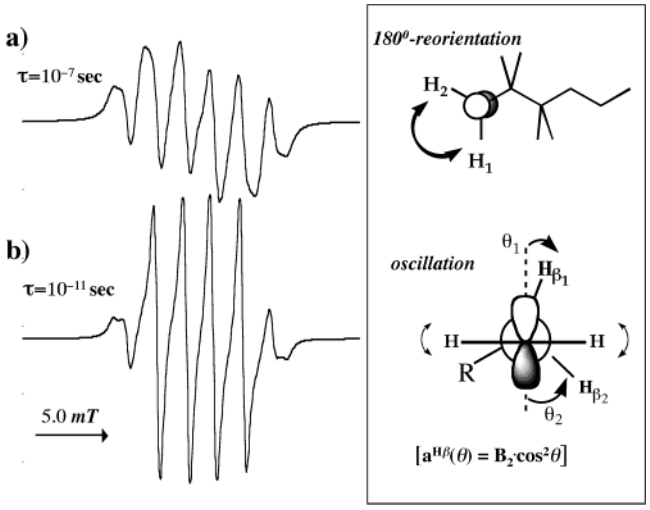

Figure 2. ESR spectra of the R_I radical simulated by the modified Bloch's equation for the two-site exchange process, which partially averages the anisotropic hyperfine tensors of the two α-C−H protons. The adopted parameters are listed in Table 1. The conformation was estimated from the $a^{H\beta}(\theta) = B_2 \cos^2 \theta$ rule. A little larger B_2 value compared with that for R_I in the polycrystalline sample at 77 K indicates that the oscillation around the C_1-C_2 bond is also suppressed in the nanochannel of MCM-41.

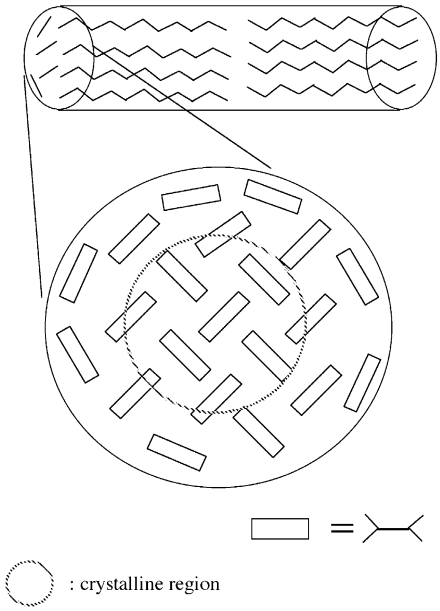

Figure 3. Schematic model for the molecular arrangement of an *n*-alkane frozen in the nanochannel. The normal crystalline part exists in the central part of the nanochannel as indicated by the dotted circle. The case of odd *n*-alkanes is shown for an example. A similar arrangement may also be expected for even *n*-alkanes, except for the central part.

From this evidence, we present a model arrangement of the long-chain alkane molecules in the nanochannel of MCM-41 as shown in Figure 3 for an odd alkane. While a small crystalline region with the normal orthorhombic arrangement may be formed in the central part, the direction of the alkane molecules near the channel wall is disrupted considerably, though they maintain the all-trans conformation. The molecules, from which free radicals giving wide eight-line spectra are generated, are

the irregularly arranged molecules distributed in the outer part of the nanochannel. In the case of even *n*-alkanes, the arrangement of molecules should be modified, accordingly, but the essential features may be the same. A fraction of the normal crystalline region becomes smaller when the diameter of the nanochannel is decreased. Since the disordered state of a long-chain *n*-alkane has not been reported so far, except for the crystalline defect formed by radiolysis[19] or segregation from the frozen $CFCl_3$ solvent,[20] we performed a model experiment. An equimolar mixture of *n*-decane, *n*-undecane, *n*-dodecane, and *n*-tridecane was rapidly quenched at 77 K in the absence of MCM-41 and γ-irradiated at 77 K. The appearance of the frozen sample was clearly different from that of the polycrystalline single component, though it was not transparent at 77 K as in the case of branched alkane. The ESR spectrum obtained for this mixture (Figure 1j) is different from those in Figure 1f−i, and also from the arithmetic sum of those, but is rather similar to those in Figure 1a−d. The resemblance of the ESR spectrum of an *n*-alkane irradiated in the MCM-41 channel with that of the quaternary mixture in the bulk indicates that the physical state of the former is also similar to that of the latter. In some cases, distorted orthorhombic phases have been detected even for the binary mixtures of *n*-alkanes.[21−23]

As the disordered state, the so-called "glassy state" is less probable because many chain-folded conformers (gauche form) are expected there, and R_{II} or R_{III} radicals must be generated via the deprotonation from the weakest C−H bonded to their gauche carbon.[17] In addition, R_I radicals may have plenty of chances to be converted into R_{II} or R_{III} by inter- or intramolecular hydrogen abstraction. It is reported that the binary mixture of *n*-$C_{24}H_{50}$ and *n*-$C_{26}H_{54}$ forms a deformed orthorhombic bilayer having a disposition different from that of the pure odd *n*-alkane, and an unusually high tension is expected between the chain ends of two molecules within a layer despite the unfolded backbones.[23] In the MCM-41 nanochannel, a highly distorted orthorhombic form with the extended conformers may also be expected for both even and odd *n*-alkanes. Considerable restriction in the motion of the terminal $^{\bullet}HCH-$ group of R_I and an excess line broadening of the observed ESR spectrum are consistent with this model. Judging from the fact that the radical in this region decays at a temperature that is lower than those both in the bulk samples and in the inner-core crystallites of the MCM system, we consider that the interactions of the outermost alkane molecules with the silicate wall must be weak. This is expected from the hydrophilic nature of SiO_2.

5. Conclusion

We conclude that long-chain *n*-alkanes cannot form the regular crystals in the MCM-41 nanochannel, whose diameter is a few nanometers. This may be rather easily accepted because the size of the nanochannel does not differ by more than one order of magnitude from the diameter of the "*n*-alkane rod", and the regular crystalline arrangement of the molecules is difficult to achieve near the wall of the nanochannel. Thus, long-chain *n*-alkanes must be solidified with a highly disordered state, which is, however, somewhat similar to the state of the regular odd *n*-alkane (distorted orthorhombic symmetry). The possibility of a glassy state with many gauche conformers[19] is dismissed. Further studies using MCM-41 with different nanochannel diameters, and also with various modifications of the nanochannel surface, must be carried out to obtain more information. It is noted here that radiation chemistry of *n*-alkanes in the nanochannel gives good information about the physical state of the molecules in the nanospace.

Acknowledgment. We thank Dr. Jun Kumagai and Mr. Shigefumi Imai of Nagoya University for allowing us to use the ^{60}Co γ-ray irradiation facility. We also thank Japan Science and Technology Corp. for the financial assistance through the Cooperative System for Supporting Priority Research. This work was partially supported by a Grant-in-Aid for Scientific Research on Priority Area "Innovative utilization of strong magnetic fields" (767, 5085208) from MEXT of Japan.

References and Notes

(1) Chang, C. D.; Silvestri, A. J. *J. Catal.* **1977**, *47*, 249.
(2) Derouane, E. G.; Dejaifve, P.; Gabelica, Z.; Vedrine, J. C. *Faraday Discuss. Chem. Soc.* **1981**, *72*, 331. Jacobs, P. A.; Martens, J. A. *Faraday Discuss. Chem. Soc.* **1981**, *72*, 354.
(3) Kresge, C. T.; Leonowicz, M. E.; Roth, W. J.; Vartuli, J. C.; Beck, J. S. *Nature* **1992**, *359*, 710. Beck, J. S.; Vartuli, J. C.; Roth, W. J.; Leonowicz, M. E.; Kresge, C. T.; Schmitt, K. D.; Chu, C. T.-W.; Olson, D. H.; Sheppard, W. W.; McCullen, S. B.; Higgins, J. B.; Schlenker, J. L. *J. Am. Chem. Soc.* **1992**, *114*, 10834.
(4) Okazaki, M.; Konishi, Y.; Toriyama, K. *Chem. Phys. Lett.* **2000**, *328*, 251−256.
(5) Konishi, Y.; Okazaki, M.; Toriyama, K.; Kasai, T. *J. Phys. Chem. B* **2001**, *105*, 9101.
(6) Okazaki, M.; Toriyama, K.; Oda, K.; Kasai, T. *Phys. Chem. Chem. Phys.* **2002**, *4*, 1201.
(7) Okazaki, M.; Toriyama, K. *J. Phys. Chem. B* **2003**, *107*, 7654.
(8) Okazaki, M.; Toriyama, K.; Sawaguchi, N.; Oda, K. *Bull. Chem. Soc. Jpn.* **2004**, *77*, 87.
(9) Hansen, E. W.; Stocker, M.; Schmidt, R. *J. Phys. Chem.* **1996**, *100*, 2195. Hansen, E. W.; Gran, H. C.; Sellevold, E. J. *J. Phys. Chem. B* **1997**, *101*, 7027. Overloop, K.; Van Gerven, L. *J. Magn. Reson., Ser. A* **1993**, *101*, 179. Ishizaki, T.; Maruyama, M.; Furukawa, Y.; Dash, J. G. *J. Cryst. Growth* **1996**, *163*, 455.
(10) Schreiber, A.; Ketelsen, I.; Findenegg, G. H. *Phys. Chem. Chem. Phys.* **2001**, *3*, 1185.
(11) Baker, J. M.; Dore, J. C.; Behrens, P. *J. Phys. Chem. B* **1997**, *101*, 6226.
(12) Toriyama, K.; Iwasaki, M.; Fukaya, M. *J. Chem. Soc., Chem. Commun.* **1982**, 1293. Fukaya, M.; Toriyama, K.; Iwasaki, M. *Radiat. Phys. Chem.* **1983**, *21*, 463.
(13) Iwasaki, M.; Toriyama, K.; Fukaya, M.; Muto, H.; Nunome, K. *J. Phys. Chem.* **1985**, *89*, 5278.
(14) Burkett, S. L.; Sims, S. D.; Mann, S. *J. Chem. Soc., Chem. Commun.* **1996**, 1367.
(15) Scherer, K. V., Jr.; Ono, T.; Yamanouchi, K.; Fernandez, R.; Henderson, P.; Goldwhite, H. *J. Am. Chem. Soc.* **1985**, *107*, 718.
(16) Toriyama, K.; Nunome, K.; Iwasaki, M. *J. Chem. Phys.* **1982**, *77*, 5891.
(17) Toriyama, K.; Nunome, K.; Iwasaki, M. *J. Phys. Chem.* **1986**, *90*, 6836. Toriyama, K.; Nunome, K.; Iwasaki, M. *J. Am. Chem. Soc.* **1987**, *109*, 4496.
(18) Fujimoto, M.; Janecka, J. *J. Chem. Phys.* **1971**, *55*, 5.
(19) Okazaki, M.; Toriyama, K. *J. Phys. Chem.* **1989**, *93*, 2883.
(20) Stienlet, D.; Luyckx, G.; Ceulemans, J. *J. Phys. Chem. B* **2002**, *106*, 10873.
(21) Denicolo, I.; Craievich, A. F.; Douset, J. *J. Chem. Phys.* **1984**, *80*, 6200.
(22) Maroncelli, H. L.; Strauss, H. L.; Syndeer, R. G. *J. Phys. Chem.* **1985**, *89*, 5260.
(23) Nyburg, S. C.; Carstensen, A.; Koh, C. A. *J. Phys. Chem. B* **2001**, *105*, 12418, and papers cited therein.